# Stabilization of Magnetohydrodynamic Modes by Surface-Magnetic-Field Topology

L. Schmitz, D. Chelf, and A. Y. Wong
*Department of Physics, University of California, Los Angeles, California 90024-1547*
(Received 4 April 1988)

The curvature-driven interchange mode is stabilized by spatially modulating the magnetic field lines at the plasma surface. This is effected by a high-order multipole field. No radial magnetic well is created, and axisymmetry is retained throughout most of the volume. The density, plasma lifetime, and pressure gradient increase by an order of magnitude in the stabilized plasma due to suppression of wave-induced radial transport. A model of wave stabilization by finite-Larmor-radius effects enhanced by the localization of wave fields is quantitatively established by computer simulation.

PACS numbers: 52.30.Bt, 52.35.Py, 52.55.Jd

We present experimental evidence to advance the concept that the interchange mode[1] can be stabilized by surface perturbation of the confining magnetic field. This control of MHD instability at the radial boundary of the plasma preserves axisymmetry throughout most of the confined volume and is easy to implement. This is useful whenever the confinement of a quiescent plasma involves a magnetic field gradient. The conventional method of stabilizing MHD modes in an absolute-minimum-$B$ configuration[2] does not lend itself to high mirror ratios, and its lack of axisymmetry can induce considerable neoclassical transport. Although our experiments were performed in a mirror device, the concept of controlling the topology of the surface field to localize and suppress MHD instabilities is general and applies to toroidal configurations. The suppression of instabilities at the plasma-vacuum interface has recently received considerable interest in connection with the $H$-mode operation of tokamaks.[3]

In our experiment the surface layer is spatially modulated by a high-order ($l=16$) multipole field produced by conducting bars surrounding the plasma [Figs. 1(a) and 1(b)]. The field-line mapping in the $(r,\theta)$ plane is illustrated in Fig. 1(c). There are moderate azimuthal as well as radial components of the magnetic field in the boundary layer [$B_\theta/B_c \leq 0.1$, $B_r/B_c \leq 0.1$, where $B_c$ is the axial field at midplane ($z=0$)]. The radial dependence of $B_\theta/B_c$ is depicted in Fig. 2(b). The width of the nonaxisymmetric surface layer is approximately $R_p/5$, where $R_p$ is the plasma radius. The surface perturbation parameter, $S_P$, used throughout the paper is the value of $B_\theta/B_c$ near the surface at radius $r_0=45$ cm, $\theta=0°$, and $z=0$. As opposed to other surface confinement schemes,[4] no radial magnetic well is formed inside the plasma and curvature drifts are not reversed. Figure 2(c) demonstrates that the specific flux tube volume,[1] $\int dL/B$, increases monotonically with radius for the range of multipole current used in our experiment.

The experiments were performed in a large vacuum chamber [Figs. 1(a) and 1(b)] at high mirror ratio ($8 \leq R \leq 35$). The magnetic field in the mirror throat, $B_{\rm thr}$, is varied between 450 and $2\times10^3$ G, while the central field, $B_c$, is maintained at 55 G. The plasma boundary is restricted by an inner wall within the multipole bars, and a circular limiter is positioned at the mirror midplane. A hydrogen plasma ($N_e \leq 3\times10^9$ cm$^{-3}$, $kT_e \leq 5$ eV, $T_e/T_i \simeq 7$, $\beta \leq 2\times10^{-4}$) is produced by launching electron-cyclotron-resonance heating (ECRH) power via a rod antenna located in the midplane close to the inner chamber wall. The ECRH resonant surfaces span the whole plasma diameter. The ECRH power is pulsed to allow for time-resolved measurements of the electron temperature and density in the plasma afterglow. Plane and cylindrical Langmuir probes are used to determine the local density $N_e(r)$, the fluctuation level $\delta N/N$, and the electron temperature $kT_e(r)$. Ion temperatures were measured with an ion-energy analyzer.

The simple mirror configuration is unstable to the curvature-driven interchange mode. Large amplitude density fluctuations ($\delta N/N \leq 0.6$) are observed throughout the plasma volume. These modes have a continuous frequency spectrum extending up to 20 kHz, peaking around 2–5 kHz. Two probes at different azimuthal positions have identified mode numbers, $m$, of 2–15. The fluctuations are well correlated across the plasma radius indicating a low radial wave number [Fig. 2(d)]. The modes are found to be flutelike perturbations ($k_\parallel=0$) by measuring the phase shift between two probes that intersect the same field line at $z=\pm L/2$ off the midplane.

A particle confinement time $\tau_p=150$–$300$ $\mu$s was derived from the decay of the ion saturation current of a cylindrical probe in the plasma afterglow. The observed value is close to the radial expansion time $\tau_{\rm fl}=5R_p/v_s$ commonly used to estimate plasma loss due to the flute instability ($v_s$ is the ion acoustic speed).[5]

Figure 2 shows the evolution of the density profile for different values of surface perturbation. The throat field is $B_{\rm thr}=550$ G and the mirror ratio is $R=10$. The experiments were performed in the afterglow 1 ms after rf shutoff to make sure that line tying due to electrons created at the ECRH layer as well as possible stabilizing

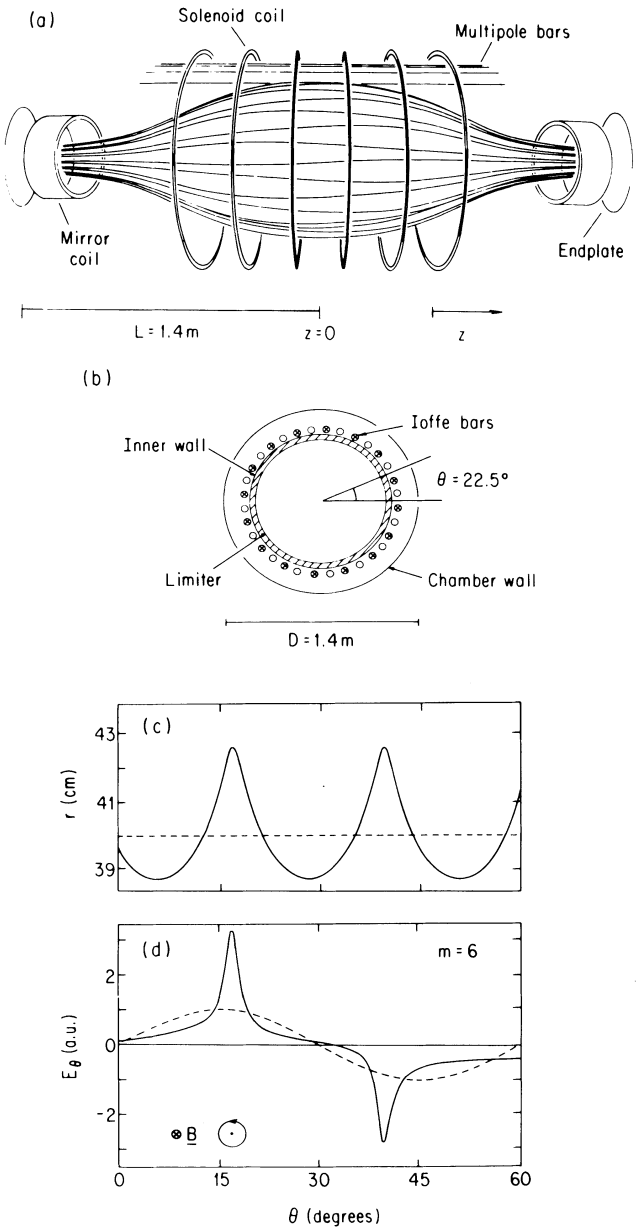


FIG. 1. (a) Schematic of mirror coil setup and $l=16$ multipole arrangement. A set of magnetic field lines demonstrating the topology of the surface layer is shown. (b) Cross-sectional view of the multipole arrangement at midplane. The bars are located at a radius of 54.5 cm; the azimuthal periodicity of the multiple field is $\theta=22.5°$. The position of the inner wall (52.5 cm) as well as the limiter (47.5 cm) is indicated. (c) Computer generated mapping of field lines in the surface layer in the $(r,\theta)$ plane. ---, flux surface at $z=L/2$ in the simple mirror configuration [$S_P=B_\theta(r_0)/B_c=0$]. ——, flux surface at $z=L/2$ with superimposed surface field ($S_P=0.035$). For this surface, $\theta$ is measured from a field line at $z=L/2$ that starts in the midplane with only azimuthal shear. (d) Azimuthal electric field of an $m=6$ mode at $z=L/2$ (the potential is kept constant along field lines). ---, $S_P=0$; ——, $S_P=0.035$. The size of the ion Larmor radius is indicated.

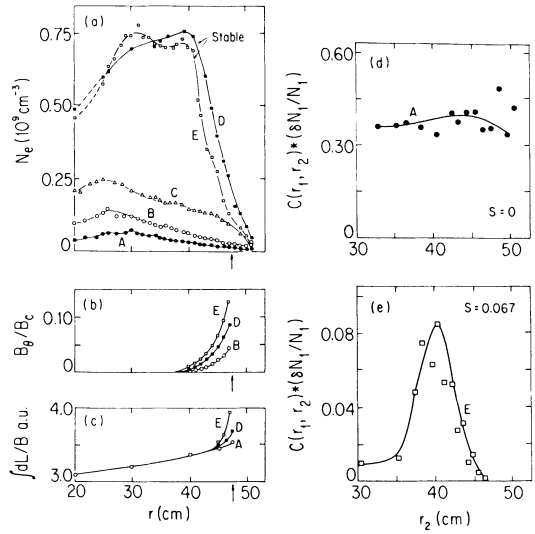


FIG. 2. (a) Radial density profile for different values of surface perturbation: $S_P=0$ (●,$A$); $S_P=0.022$ (○,$B$); $S_P=0.034$ (△,$C$); $S_P=0.045$ (■,$D$); and $S_P=0.067$ (□,$E$). (b) $B_\theta/B_c$ as a function of radius for $S_P=0.022$ (○,$B$); $S_P=0.045$ (■,$D$); and $S_P=0.067$ (□,$E$). (c) Specific flux tube volume $\int dL/B$ as a function of radius for the simple mirror configuration $S_P=0$ (●,$A$), and with superimposed surface field $S_P=0.045$ (■,$D$), and $S_P=0.067$ (□,$E$). The data are mapped to the midplane ($\theta=0$, $z=0$). The position of the limiter is indicated by an arrow. (d) Radial correlation of flute modes in the surface layer for the frequency range $3\leq f\leq 10$ kHz in the simple mirror configuration $S_P=0$ (●,$A$).

$$C(r_1,r_2)=\langle\delta N(r_1)\delta N(r_2)\rangle/\langle\delta N(r_1)\rangle\langle\delta N(r_2)\rangle$$

is determined from the ion saturation current of two probes located at $r_1$ and $r_2$ ($\theta=5.625°$, $z_1=L/2$, and $z_2=0$). Shown is the correlation function $C(r_1,r_2)$ multiplied by the fluctuation level $\delta N_1/N_1$. The stationary probe is kept at $r_1=39$ cm ($B_{\rm thr}=5.5\times10^{-2}$ T, $R=10$). All radii are mapped to the midplane. (e) Radial correlation with superimposed surface perturbation $S_P=0.067$ (□,$E$).

effects due to hot electrons[6] do not have to be taken into account. In the simple (unstable) mirror configuration [$S_P=B_\theta(r_0)/B_c=0$] the time-averaged density gradient is flattened as a result of intense plasma convection from low-frequency turbulence. As soon as the surface perturbation exceeds the critical strength ($S_P\geq 0.045$) a stable surface layer is created, and a negative pressure gradient can be supported at the plasma boundary. The electron temperature shows no significant radial variation so that the pressure profile can be approximated by the density profile. The density increases by an order of magnitude as a result of improved radial confinement, and a hollow profile develops in the core plasma. This is consistent with the Rosenbluth-Longmire energy criterion, since $\int dL/B$ is increasing with radius [Fig. 2(c)]. In the stable plasma the density profile peaks close to the boundary of the perturbed surface layer.

The radial correlation of the unstable modes is determined by comparing the density fluctuations measured by two probes located at the same azimuth. One probe is kept stationary, while the second probe is moved to different radii. The correlation function $C=\langle\delta n_1\delta n_2\rangle/\langle\delta n_1\rangle\langle\delta n_2\rangle$ is obtained by multiplying the fluctuating part of the ion saturation currents and using a boxcar integrator for averaging. The measurement is performed in the afterglow 1 ms after rf switchoff, and a high pass filter is employed to suppress the dc component of the ion saturation current. The results are presented in Fig. 2. For $S_P=B_\theta(r_0)/B_c=0$ the modes are well correlated over a large radial distance. For $S_P\geq 0.045$ the modes are localized radially and of significantly lower amplitude. The width of the correlation function is found to vary inversely with the amount of surface perturbation at the radius of the fixed probe.

Figure 3 shows the density fluctuation level $\delta N/N$ (integrated over all modes), the line-averaged density $\int N_e\,dr/R_p$, the particle confinement time $\tau_p$, and the growth rate obtained from computer simulation $\gamma$ as a function of $S_P$. Stabilizing effects are observed to set in for $S_P\geq 0.015$. The average density and the confinement time increase substantially due to suppression of flute-induced radial losses. A saturation of the confinement time is observed for $S_P\simeq 0.045$, when the fluctuation level has dropped to $\delta N/N\simeq 0.1$. For the plasma parameters of our experiment, the ion collision rate (mainly determined by small-angle Coulomb collisions) is larger than the bounce rate between the mirror throats so that the axial loss time is expected to follow the collisional scaling, $\tau_c\simeq RL/2v_s$.[7] Figure 3(c) demonstrates that $\tau_p$ approaches $\tau_c$ in the stabilized plasma ($\tau_c$ was evaluated using the electron temperature measured in the afterglow). In the stabilized regime, a linear dependence of $\tau_p$ on mirror ratio is found over a range of $8\leq R\leq 35$. This indicates that radial losses are negligible as compared to axial losses, which is in agreement with a simple estimate of the radial plasma loss by diffusion.

We wish to point out that finite-Larmor-radius (FLR) effects,[8] in the absence of the surface field, are expected to stabilize only high-azimuthal mode numbers $m\geq 25$, because the ion Larmor radius, $\rho_i$, is small compared to the plasma radius ($\rho_i/R_p\simeq 0.04$). As large amplitude low-order modes are actually found in the experiment without surface stabilization, there is obviously no significant line tying due to the conducting end plates, consistent with the theory of Liebermann and Wong.[9]

The experimental data as well as a computer simulation suggest that the following physical picture explains the concept of flute stabilization by surface perturbation. In the simple mirror configuration, magnetic field lines form smooth circular flux surfaces [Fig. 1(c)]. In the presence of the surface field, the flux surfaces remain nearly circular at $z=0$, but map into a cycloidal pattern

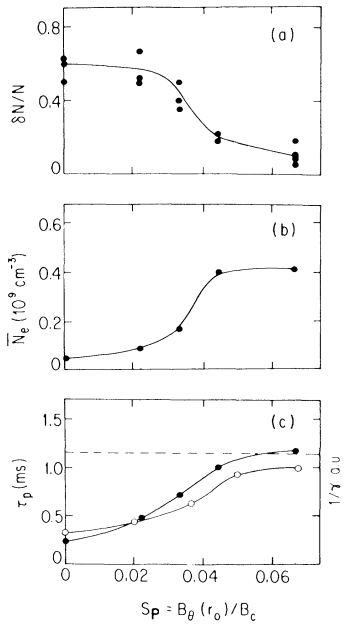


FIG. 3. (a) Fluctuation level $\delta N/N$ averaged over the radius; (b) line-averaged density $\bar{N}_e=\int N_e\,dr/R_p$; (c) plasma lifetime $\tau_p$ as a function of $S_P=B_\theta(r_0)/B_c$ ($B_{\rm thr}=5.5\times10^{-2}$ T, $R=10$). The dashed line corresponds to $\tau_p=RL/2v_s$. The data are taken after the plasma production has been turned off. Included in (c) is the inverse growth rate, $1/\gamma$, derived from computer simulation for a plasma at a radius of $r_0$ as a function of $S_P$ (○). The ion Larmor radius corresponds to the experimental value.

off the midplane. This is illustrated in Fig. 1(c) for $z=L/2$. The wave potential of the interchange mode is essentially constant along the field lines ($k_\parallel\simeq 0$). The spatial distribution of the wave potential, therefore, follows closely the distribution of field lines and adopts the spatial periodicity of the surface field. Thus the azimuthal electric field is enhanced where the field lines bunch in azimuthal direction. This is illustrated in Fig. 1(d) for the example of an $m=6$ mode. Close to the tips of the cycloids the scale length of the electric field is comparable to the ion Larmor radius as indicated in the figure, so that significant FLR stabilization is expected.

The computer simulation used to verify this physical picture is a 2D electrostatic particle push code with rectangular geometry, uniform magnetic field, uniform gravitational field, and $2.5\times10^4$ particles. The simulation yields the linear growth rate of the gravitational interchange instability. The interchange can be simulated by a 2D code because the electric potential is constant along magnetic field lines. The surface magnetic field causes the field lines of a flux tube to bunch together on one side of the midplane and diverge on the other side. This effect is accounted for in the computer simulation by representing each side of the midplane by a 2D plasma cross section. The charge distributions from both

sides are then superimposed in the midplane. The electric potential from the total charge distribution in the midplane is then mapped along the magnetic field lines to the two sets of particles, and the particles are advanced.

Figure 3(c) shows the inverse growth rate, $1/\gamma$, derived from the electric field energy in the computer simulation, as a function of the surface perturbation, $S_P$. This simulation shows that FLR effects enhanced by forced wave localization can account for a factor of 3 reduction in the interchange growth rate. Here the ratio of thermal ion Larmor radius to multipole periodicity is 1:16, which approximates the experimental conditions. For an ion Larmor radius half as large, $\gamma$ is almost uneffected by $S_P$, which demonstrates the need for both FLR and a multipole field to reduce the growth of the interchange wave. Experimentally, the density profile curves $D$ and $E$ of Fig. 2(a) show that the plasma edge develops at a critical value of $B_\theta/B_c$, which moves inward as $S_P$ increases. $B_\theta/B_c$ is approximately 0.05 at the steepest density gradient for both $S_P=0.045$ and 0.067. This critical value of $B_\theta/B_c$ in the experiment matches well with the saturation level of $S_P$ (also about 0.05) derived from computer simulation.

We have eliminated wall stabilization on the following grounds. Wall stabilization, to be effective, requires the plasma boundary to be an equipotential surface and the density to be sufficiently high at this surface.[10,11] Experimentally, however, at the radial boundary we find a wall sheath ($e\phi/kT_e \simeq 2$) and fluctuation levels comparable to those well inside the plasma for both the stable and unstable regimes. The ratio of wall to peak density is larger in the unstable simple mirror configuration than in the stable multipole configuration. The density at the wall or limiter is a factor 3–5 less than that predicted theoretically by Lehnert,[10] Fornaca,[11] and Caponi, Cohen, and Freis,[12] for the appreciable reduction of the growth rate of low-order interchange modes. We have therefore eliminated wall stabilization as a possible explanation.

We wish to acknowledge the contribution of Dr. G. Dimonte in the early phase of the experiment. We are grateful to Dr. V. Decyk for providing the particle code used in the simulation. This research is supported by the National Science Foundation under Grant No. PHY85-02490 and University of California at Los Angeles Academic Senate Grant No. 2171.

[1]M. N. Rosenbluth and C. L. Longmire, Ann. Phys. (N.Y.) **1**, 120 (1957).

[2]Y. B. Gott, M. S. Ioffe, and V. G. Telkovsky, in *Proceedings of the Conference on Plasma Physics and Controlled Nuclear Fusion Research, Salzburg, Austria, 1961* (IAEA, Vienna, 1963), p. 1045.

[3]C. M. Bishop, Nucl. Fusion **26**, 1063 (1986).

[4]J. R. Ferron, G. Dimonte, A. Y. Wong, and B. Leikind, Phys. Fluids **26**, 2227 (1983); B. Lane, R. S. Post, and J. Kesner, Nucl. Fusion **27**, 277 (1987).

[5]LLNL Report No. UCAR 10049-80-Rev 1, 1980, edited by B. I. Cohen (unpublished).

[6]H. L. Berk, J. W. Van Dam, and M. N. Rosenbluth, Phys. Fluids **26**, 201 (1983).

[7]A. Makhijani, A. J. Lichtenberg, M. A. Liebermann, and B. Grant Logan, Phys. Fluids **17**, 1291 (1974).

[8]M. N. Rosenbluth, N. A. Krall, and N. Rostoker, Nucl. Fusion Suppl. **1**, 143 (1962).

[9]M. A. Liebermann and S. L. Wong, Plasma Phys. **19**, 745 (1977).

[10]B. Lehnert, Phys. Fluids **9**, 1367 (1966).

[11]S. W. Fornaca, thesis, University of California, Irvine, 1980 (unpublished), p. 78.

[12]M. A. Caponi, B. I. Cohen, and R. P. Freis, Phys. Fluids **30**, 1410 (1987).